CHARACTERISTICS OF THE MEAN FLOW OVER A SIMULATED URBAN AREA

CARACTERISTIQUES D'ECOULEMENT MOYEN SUR UNE SURFACE URBAINE SIMULEE

T. Kawatani* - J. E. Cermak** - R. N. Meroney***

Summary

A study of the mean flow field over high roughness elements was carried out in a wind tunnel using roughness elements consisting of pegs 9 cm high and 0.48 cm in diameter, arranged in four geometrical patterns. A power law which is commonly applied to estimate the mean velocity over urban areas was adapted to analyze the mean velocity data obtained in this experimental work. The dependence of the exponent in the power law on the roughness density was examined. A similarity velocity profile was obtained for the flow within the internal boundary layer using the internal boundary-layer thickness and the velocity at that height as scaling parameters.

Introduction

The flow in the atmospheric boundary layer is strongly affected by underlying roughness conditions. Particularly, when a change in the surface-roughness conditions exist, the interrelation between the velocity field and ground roughness becomes more complicated. A better knowledge of the interrelationship between the mean velocity distribution and roughness conditions may be valuable for estimating the wind loads on buildings and/or structures. Theoretical analysis, however, is extremely difficult due to the complexity involved in the problem. Hence, detailed experimental study is necessary. Field measurements are inherently difficult because of the continuous weather change and the high cost in setting up measurement stations. On the other hand, an appropriate wind tunnel can now provide satisfactory conditions for simulating the atmospheric boundary layer.

The prime objective of this experiment is to investigate the evolution of the mean velocity above high roughness elements. The mean velocity and the growth of the internal boundary layer are examined by employing the power-law relationships.

Experimental design

The aim of this study was to study the mean velocity variation over a highly rough surface which might simulate an urban area or a wooded area. The usefulness of wind tunnels for simulating the atmospheric boundary layer has been well verified. An extensive discussion about simulation of the atmospheric flow field by wind-tunnel flow can be found in Refs. [1] and [2].

The experiment reported herein was carried out in the low speed Meteorological Wind Tunnel in the Fluid Dynamics and Diffusion Laboratory at Colorado State University [3]. Previous simulation results of urban and forest-canopy meteorology conducted in this wind tunnel have been reported in Refs. [4], [5], [6], [7] and [8].

---

* Research Assistant, Department of Civil Engineering, Colorado State University, Fort Collins, Colorado

** Professor-in-Charge, Fluid Mechanics Program, Colorado State University, Fort Collins, Colorado

*** Associate Professor, Colorado State University, Department of Civil Engineering, Fort Collins, Colorado

Roughness

The roughness surface consisted of pegs 9 cm high and 0.48 cm in diameter. This surface was 1100 cm long and 183 cm wide. The pegs were arranged in the following four patterns:

(1) Case S(I): The pegs were spaced 2.54 cm in both longitudinal and lateral directions.
(2) Case S(II): The pegs were spaced 5.08 cm in both longitudinal and lateral directions.
(3) Case D(I): One peg was inserted at the center of a square formed by four pegs in Case S(I). Both longitudinal and lateral rows of pegs were 1.27 cm apart. That is, pegs were spaced 1.80 cm on the diagonal.
(4) Case D(II): One peg was inserted at the center of a square formed by four pegs in Case S(II). Both longitudinal and lateral rows of pegs were 2.54 cm apart. Pegs were spaced 3.60 cm on the diagonal.

Area roughness density σ_A is defined as the ratio of the surface area occupied by the pegs to total roughness-surface area. The values of σ_A are 0.056 for Case D(I), 0.028 for S(I), 0.014 for D(II) and 0.007 for S(II).

Wind tunnel

The meteorological Wind Tunnel is a closed circuit wind tunnel with a 26 m long test section and a cross-section of 2 x 2 m. Air speed up to about 36 m/s can be obtained.

The rough surface of pegs started 15 m downstream of the test-section entrance.

To simulate the atmospheric shear layer a thick turbulent boundary layer was generated by gravel placed in the contraction section. An additional turbulence generator made from flexible plastic strips was placed over the first 3 m of the test section [6].

A photograph of the peg roughness installed in the wind tunnel is displayed in Fig. 1.

Mean velocity measurement

The experiment was conducted at a constant free-stream velocity of 12 m/s. The latter was obtained by adjusting the height of the tunnel ceiling sectionally.

The mean velocity was measured by a pitot-static tube and a hot-wire anemometer. The turbulence level is very high in and immediately above the roughness e.g., 40 to 50% of the local mean velocity. The accuracy of a hot-wire anemometer for mean velocity measurements is expected to be insensitive to such high turbulence [9]. Thus, the mean velocity measurements up to 60 cm from the floor were made by a hot-wire anemometer, and above 60 cm a pitot-tube was utilized. In Cases S(I) and S(II), the velocity was measured at the center of a square formed by four pegs. In Cases D(I) and D(II), one peg was removed and the measurement was made at this position.

Experimental results

The variation of the free-stream velocity along the rough surface was found to be less than 2 percent.

In presenting the results, the longitudinal distance, x, is measured from the leading edge of the rough surface in the downwind direction. The vertical distance, z, is measured from the floor.

The mean velocity profile within the atmospheric boundary layer can be described by a power law, i.e., $U \alpha z^{\alpha}$. The value of α for the velocity profile at $x = -1$ m is approximately 0.175. For flat open country a value of 0.16 has been suggested [10]. The value of α for the upstream velocity is only about 10% larger than the suggested value for open country. Consequently, the velocity distribution in the atmospheric surface layer over flat surface was simulated adequately by the upstream flow.

The velocity distribution in the atmospheric shear layer is usually expressed by either a logarithmic law or a power law. For micrometeorological problems, the former is used more frequently than the latter. However, when the surface roughness is high, the application of a logarithmic law to describe the wind profile becomes extremely difficult. This is primarily because the prediction of two similarity parameters, i.e., the friction velocity and the roughness length, becomes difficult and hence inaccurate [11, 12]. On the other hand, to estimate the wind load on buildings and/or structures, a power law is convenient because of its simplicity. The power law to represent the velocity profile throughout the atmospheric boundary layer is written by [10]

$$\frac{U}{U_G} = \left(\frac{z}{z_G}\right)^{\alpha} \tag{1}$$

where U_G denotes the geostrophic wind speed and z_G is the height at which U_G is attained. For simulating the atmospheric boundary layer in a wind tunnel U_G and z_G can be replaced by the free-stream velocity U_∞ and the boundary-layer thickness δ, respectively [13]. Then, Eq. (1) is written as

$$\frac{U}{U_\infty} = \left(\frac{z}{\delta}\right)^{\alpha} \tag{2}$$

It is important to note that the roughness element used in this work is extremely high, i.e., 8 to 12% of the boundary-layer thickness. Within the roughness ($z \leq h$), the flow is highly turbulent and a two-dimensional wake is generated behind each peg [4, 7]. Immediately above the roughness, three-dimensional wake is produced due to the flow separation from the top of each roughness element [7]. Beyond the three-dimensional wake domain, a two-dimensional turbulent boundary-layer flow is observed. Equation (2) is applicable to the flow in the last domain. Therefore, to express the velocity profile above high roughness elements, Eq. (2) is modified into the form [6]

$$\frac{U}{U_\infty} = \left(\frac{z-h}{\delta-h}\right)^{\alpha} \qquad (z > h) \tag{3}$$

where h is the roughness height.

In the analysis of vertical velocity distributions, horizontal homogeneity of the surface roughness is commonly assumed so that the flow characteristics throughout the boundary layer are determined by the underlying roughness only. The flow in such a stage is called a fully developed flow. When the fully developed flow encounters the change in the roughness conditions the influence of new roughness on the flow is confined to a layer next to the ground, i.e., the internal boundary layer [14]. The internal boundary layer grows in depth with downwind distance. Thus, near the roughness change, the flow is affected by both upstream and new roughness conditions. This flow domain is called a transition region.

The velocity profiles in the fully developed flow region for Cases D(I), S(I), D(II) and S(II) are shown in Figs. 2a, b, c and d, respectively. The boundary layer thickness was defined as the distance from the wall where $U/U_\infty = 0.99$. For the sake of comparison, the power-law profiles which envelope the measured velocities are also displayed. The variation of the exponent due to the roughness-density change is clearly observed. Samples of the change in the exponent for different roughness conditions are provided by Fig. 3 for wind-tunnel data [15] and by Fig. 4 for field data [16]. The former is a case where the spacing of fences 2.54 cm high was varied. The latter was obtained in a rough and irregular area. Close examination of Figs. 2a to d and 3 shows that near the roughness top the vertical velocity gradient, dU/dz, for the measured velocity profiles is larger than for the profile given by Eq. (3). As the outer edge of the boundary layer is approached, the situation is reversed. A similar result is observed in Ref. [13]. Note that the velocity profiles expressed by Eqs. (1), (2), and (3) do not have zero velocity gradient at the outer edge of the boundary layer. In reality, the velocity within the boundary layer should approach asymptotically to the geostrophic wind speed or to the free-stream

velocity with increasing vertical distance. It is observed that the change in the measured mean velocity from $0.9\,U_\infty$ to U_∞ takes place over a vertical distance extending from about $0.75\,\delta$ to δ. Therefore, if the length scale z_G or δ is defined as the height where $U = 0.9\,U_G$ or $0.9\,U_\infty$, a better agreement between the measured velocity profile and one expressed by Eq. (1), (2) or (3) may be obtained.

The velocity profiles at various downwind distance for Case S(I) are shown according to Eq. (3) in Fig. 5, where δ is the height for $U/U_\infty = 0.99$. At a certain height, each velocity profile merges into the profile at $x = 0$ m. This height is defined as the internal boundary-layer thickness, denoted by δ_i. The growth of the internal boundary layer for four cases is displayed in Fig. 6. The internal boundary-layer thickness increases almost linearly as x increases. The latter becomes practically constant when the flow is fully developed. The extent of the transition region, designated by x_T, becomes shorter as the roughness density increases.

In order to express the velocity profiles in the transition region, Eq. (3) is modified into the form

$$\frac{U}{U_i} = \left(\frac{z-h}{\delta_i-h}\right)^{\beta} \tag{4}$$

where U_i denotes the mean velocity at δ_i. According to Eq. (4), the velocity profiles within the internal boundary layer are presented in Figs. 7a, b, c and d for Cases D(I), S(I), D(II) and S(II), respectively. The numerical values of δ_i U_i and β are summarized below:

		Case D(I)			Case S(I)			Case D(II)			Case S(II)		
x (m)	$\tilde{x}$	$\tilde{\delta}_i$	$\tilde{U}_i$	β	$\tilde{\delta}_i$	$\tilde{U}_i$	β	$\tilde{\delta}_i$	$\tilde{U}_i$	β	$\tilde{\delta}_i$	$\tilde{U}_i$	β
0.5	5.5	2.3	0.70	0.840	---	----	-----	---	----	-----	---	----	---
1.0	11.1	2.9	0.74	0.735	2.3	0.72	0.585	2.3	0.76	0.447	2.3	0.77	0.33
1.5	16.6	---	----	-----	---	----	-----	2.7	0.78	0.447	2.6	0.78	0.33
2.0	22.2	4.1	0.80	0.585	3.6	0.78	0.447	3.6	0.80	0.447	3.1	0.79	0.33
3.0	33.3	5.3	0.85	0.535	---	----	-----	4.3	0.83	0.447	---	----	----
4.0	44.4	6.3	0.90	0.535	5.4	0.86	0.447	5.4	0.86	0.447	4.0	0.81	0.33
5.0	55.5	7.5	0.93	0.535	---	----	-----	---	----	-----	---	----	----
6.0	66.6	7.4	0.93	0.535	7.1	0.90	0.447	8.4	0.93	0.447	6.0	0.87	0.33
7.0	77.7	7.5	0.93	0.535	---	----	-----	---	----	-----	---	----	----
7.5	83.3	---	----	-----	7.1	0.90	0.447	---	----	-----	---	----	----
8.0	88.8	---	----	-----	---	----	-----	8.6	0.93	0.447	8.6	0.95	0.33

In the above table, $\tilde{x} = x/h$ $\tilde{\delta}_i = \delta_i/h$ and $\tilde{U}_i = U_i/U_\infty$ where $h = 9$ cm and $U_\infty = 12$ m/s. In Cases D(II) and S(II), all the measured velocity profiles within the internal boundary layer collapse on a single curve. In cases D(I) and S(I), for $x \leq 2$ m ($x/h \leq 22.2$), similar velocity profiles are also obtained. These results reveal the validity of δ_i and U_i as similarity parameters. Within the very beginning of the transition regions for both D(I) and S(I) cases, the velocity profiles exhibit a deviation from the similarity profile obtained at distances farther downstream. Notice that in Case S(I) the ratio of a peg diameter to the spacing, i.e., the ratio of the area of pegs projected in the x direction to total frontal area of roughness, is about 0.19. In Case D(I), since the first lateral row of pegs and the second one are close, the aforementioned ratio based on the spacing distance measured diagonally is approximately 0.27. In these cases, the frontal area of the roughness can be regarded as a step obstruction or a permeable fence. Hence, the flow field in the immediate vicinity of the leading edge of the rough surface is considered similar to a wake generated by a fence or a corner of a building. The aforementioned deviation of the velocity profiles from the similarity profile might be attributed to these initial fence-wake flow characteristics.

It is noteworthy that once the internal boundary-layer thickness is estimated the mean velocity U_i, which is the velocity scale in Eq. (4), could be evaluated substituting δ_i into z of Eq. (3) for $x = 0$ m.

In order to assess the efficiency of roughness in reducing the mean velocity, the volumetric density of roughness, σ_V, is defined as $\sigma_V = (\sigma_A\, h)/\delta_o$, where δ_o is the boundary-layer thickness at $x = 0$ m. The value of σ_V for Cases D(I), S(I), D(II) and S(II) are 7.0×10^{-3}, 3.5×10^{-3}, 1.75×10^{-3}, and 0.88×10^{-3}, respectively. Consider a hypothetical case where houses 10 m high occupy 50% of the total residential area and the height of the atmospheric shear layer is 1000 m [17]. The value of σ_V for this case is 5.0×10^{-3} which locates between Cases D(I) and S(I). In Fig. 8, the variation of β in Eq. (4) with σ_V and the extent of the transition region are shown. The value of β for a similarity profile increase with increasing density. As shown by the broken line, the value of β should approach to a value of 0.16 for sufficiently small roughness density.

Acknowledgement

The work reported herein was supported by the Integrated Army Meteorological Wind-Tunnel Research Program under Grant DA-AMC-28-043-65-G20. This support together with support in preparing this paper by Project THEMIS, Office of Naval Research, Contract N00014-68-A-0493-0001 are gratefully acknowledged.

References

[1] Cermak, J. E., Sandborn, V. A., Plate, E. J., Binder, G. H., Chuang, H., Meroney, R. N. and Ito, S.: "Simulation of atmospheric motion by wind tunnel flow," Fluid Dynamics and Diffusion Laboratory, Colorado State University, Fort Collins, Colorado, TR CER66JEC-VAS-EJP-GHB-RNM-SI17. (1966).

[2] McVehil, G. E., Ludwig, G. R. and Sundaram, T. R.: "On the feasibility of modeling small-scale atmospheric motions," Cornell Aero. Lab., Buffalo, N.Y. TR ZB-23228-P-1. (1967).

[3] Plate, E. J. and Cermak, J. E.: "Micrometeorological wind tunnel facility," Fluid Dynamics and Diffusion Laboratory, Colorado State University, Fort Collins, Colorado, TR CER63EJP-JEC9. (1963).

[4] Kawatani, T. and Meroney, R. N.: "The structure of canopy flow field," Fluid Dynamics and Diffusion Laboratory, Colorado State University, Fort Collins, Colorado, TR CER67-68TK66. (1968).

[5] Cermak, J. E. and Arya, S. P. S.: "Problems of atmospheric shear flows and their laboratory simulation," Boundary-layer Meteorology, Vol. 1, No. 1, pp. 40-60. (1970).

[6] Plate, E. J. and Quaraishi, A. A.: "Modeling of velocity distributions inside and above tall crops," Journal of Applied Meteorology, Vol. 4, pp. 400-408. (1965).

[7] Yano, M.: "The turbulent diffusion in a simulated vegetative cover," Ph.D. Dissertation, Fluid Mechanics Program, Colorado State University, Fort Collins, Colorado. (1966).

[8] Sadeh, W. Z., Cermak, J. E. and Hsi, G.: "A study of wind loading on tall structures -- Atlantic-Richfield Plaza Buildings," Fluid Dynamics and Diffusion Laboratory, Colorado State University, Fort Collins, Colorado, TR CER68-69WZS-JEC-GH36. (1969).

[9] Hinze, J. E.: "Turbulence," McGraw-Hill Book Company, Inc. (1959).

[10] Davenport, A. G.: "The relationship of wind structure to wind loading," Proceedings of Symposium on Wind Effects on Buildings and Structures, Teddington, Middlesex, Vol. 1, pp. 53-102. (1963).

[11] Hanna, S. R.: "Turbulence and diffusion in the atmospheric boundary layer over urban areas," Seminar presented at Syracuse University. (1970).

[12] Sadeh, W. Z., Cermak, J. E. and Kawatani, T.: "Flow over high roughness elements," Boundary-Layer Meteorology, Vol. 1, pp. 321-344. (1971).

[13] Cermak, J. E.: "Determination of wind loading on structural models in wind-tunnel simulated winds," Proceedings of Symposium on Wind Effects on High-Rise Buildings, Northwestern University, Evanston, Illinois. (1970).

[14] Elliott, W. P.; "The growth of the atmospheric internal boundary layer," Transactions, American Geophysical Union, Vol. 39, No. 6, pp. 1048-1054. (1958).
[15] Kung, R. J.: "Boundary layer development over equally spaced fences," Ph.D. Dissertation, Fluid Mechanics Program, Colorado State University, Fort Collins, Colorado. (1970).
[16] Slade, D. H.: "Wind measurement on a tall tower in rough and inhomogeneous terrain," Journal of Applied Meteorology, Vol. 8, pp. 293-297. (1969).
[17] Haltiner, G. J. and Martin, F. L.: "Dynamical and Physical Meteorology," McGraw-Hill Book Company. (1957).

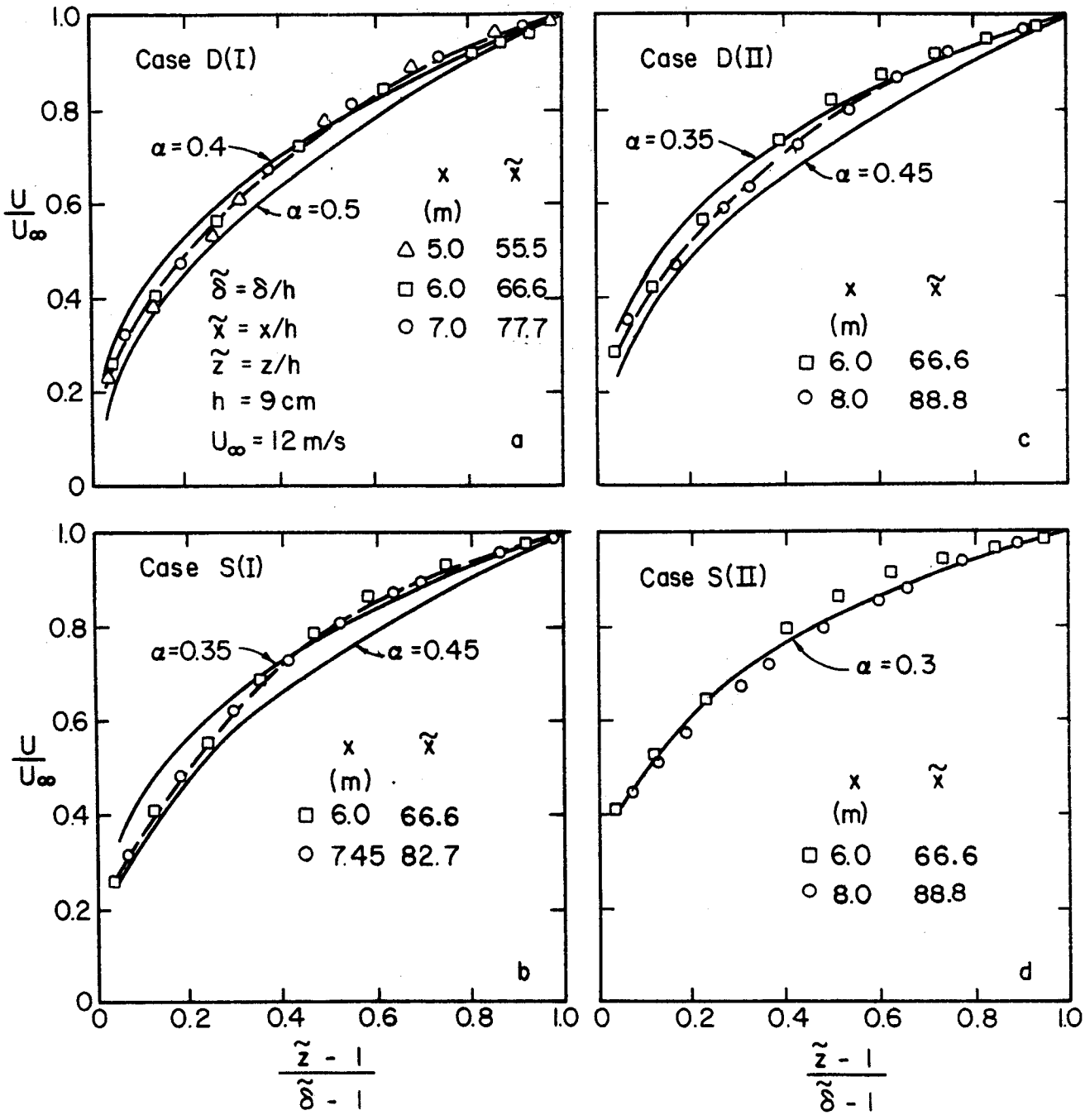

Fig. 2 - Mean velocity profiles in the fully developed flow domain.

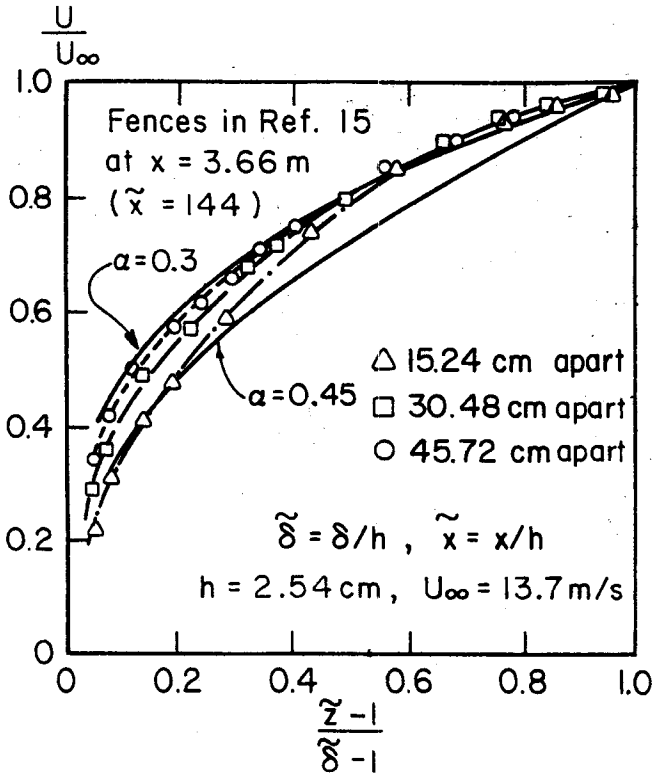

Fig. 3 - Mean velocity profiles over fences.

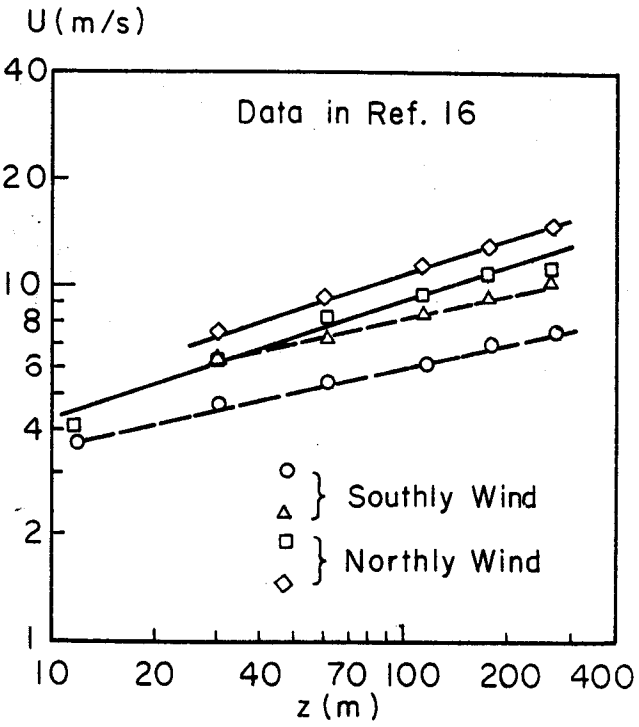

Fig. 4 - Mean velocity profiles over a rough and irregular area.

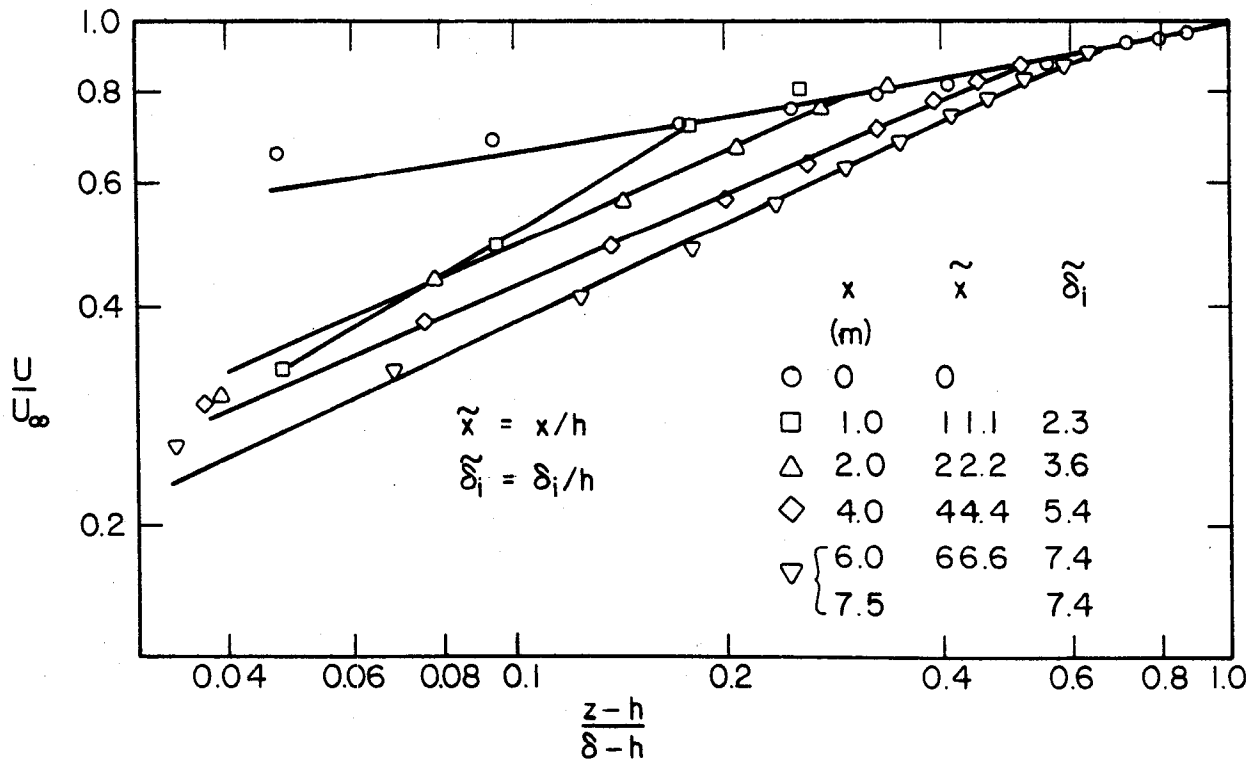

Fig. 5 - Change in the mean velocity profiles in the x-direction, Case S(I).

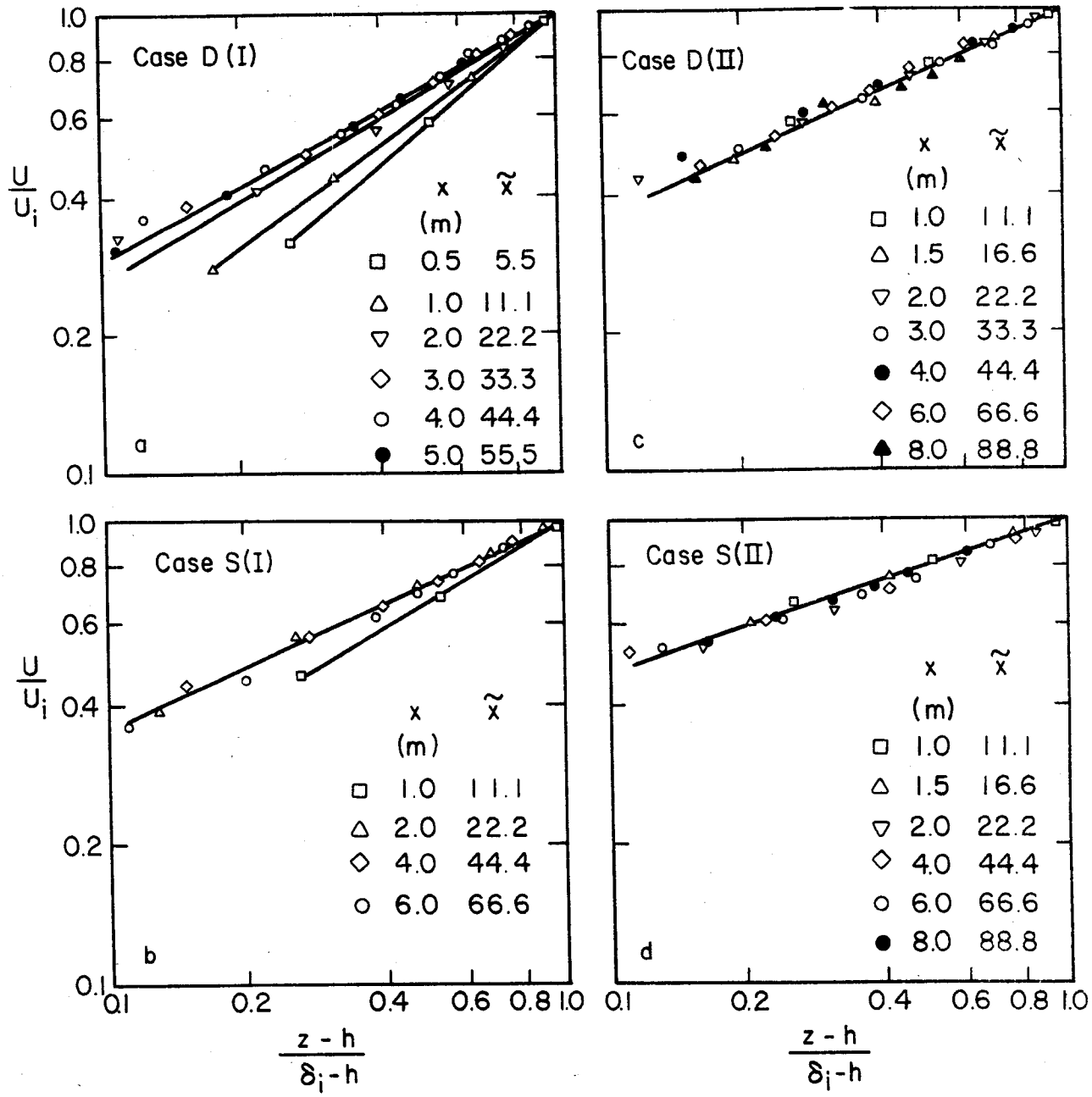

Fig. 7 - Mean velocity profiles within the internal boundary layer.

Fig. 6 is on the next page.

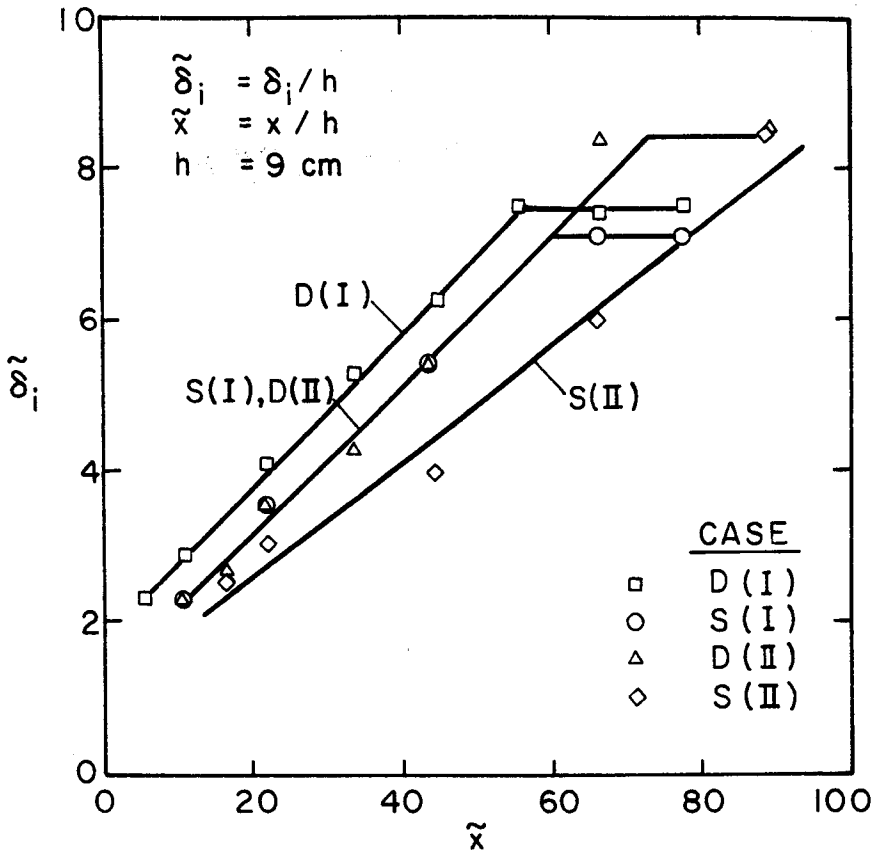

Fig. 6 - Growth of the internal boundary layer.

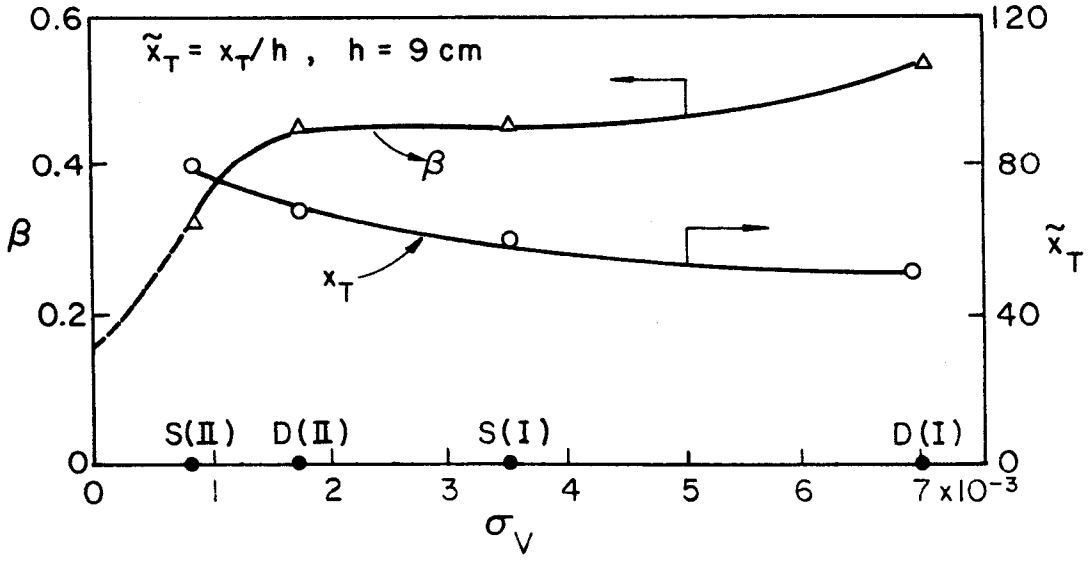

Fig. 8 - Variation of the exponent in Eq.(4) and the extent of the transition region with the roughness density.